www.czasopisma.pan.pl PAN www.journals.pan.pl

Opto-Electronics Review 25 (2017) 242–250

Contents lists available at ScienceDirect

Opto-Electronics Review

journal homepage: http://www.journals.elsevier.com/opto-electronics review

Local crystalline structure of multinary semiconducting alloys: Random *vs.* ordered distributions

A. Kisiel [a,*], B.V. Robouch [b], A. Marcelli [b,c]

[a] *Instytut Fizyki im.Mariana Smoluchowskiego, Uniwersytet Jagielloński, ul. S. Łojasiewicza 11, 30- 348, Cracow, Poland*
[b] *INFN – Laboratori Nazionali Frascati, via E. Fermi 40, CP 13, 00044 Frascati (RM), Italy*
[c] *Rome International Center for Materials Science Superstripes (RICMASS), Via dei Sabelli 119A, 00185, Roma, Italy, Italy*

ARTICLE INFO

Article history:
Received 21 January 2017
Accepted 24 June 2017
Available online 17 August 2017

Keywords:
Local crystal structure
Tetrahedron ordered semiconductors
Statistical model
EXAFS
FTIR
Site occupation preferences
Sizes and shape of elemental tetrahedra

ABSTRACT

A description of the status of the art of experimental and theoretical investigations of local crystalline structures of tetrahedron ordered ternary and quaternary semiconducting alloys is presented. Experimental EXAFS data and FTIR analysis are summarized and analyzed using both the *Rigid Network Cations* theoretical model and the *Strained-tetrahedra* model. Internal preferences of ion pairs in ternary and quaternary alloys are discussed. Several ternary systems of different structures show ideal quasi-canonical Bernoulli distributions, while others are characterized by extreme preferences in which one, several or even all configurations are depressed or even lacking. The results demonstrate that the validity of the Bernoulli distribution is limited and not fulfilled in many systems. This article is an expanded version of the scientific reports presented at the International Conference on Semiconductor Nanostructures for Optoelectronics and Biosensors 2016 ICSeNOB2016, May 22–25, 2016, Rzeszow, Poland.

Contents

1. Introduction

Melting and subsequently crystallizing two or more miscible chemical compounds lead to solid solutions or alloys. Combining in various proportions two binary compounds containing cations (A, B and/or C) and anions (X, Y and/or Z) result in an unlimited number of ternary (ABX or AXZ) or quaternary (ABXY, ABCX or AXYZ) alloys with continuously varying physical properties of particular interest for semiconductor physics. Binary semiconductor compounds with cations from Column II or III of the Mendeleev table and anions from Column VI or V usually crystallize as tetrahedron coordinated *fcc* cubic zincblende B3 (sphalerite) or hexagonal wurtzite B4 structures. Both structures are characterized by the tetrahedral spatial ordering: a cation\anion at the center of the tetrahedron surrounded by four atoms anions\cations at the four corners of the tetrahedron. The ternary alloys contain five distinct elementary tetrahedra $(T_k)_{k=0,4}$ each. The unit cell of their binary compounds is diatomic. Each atom in the crystal lattice in the first zone of nearest neighbours (NN) with coordination number N_1 of four and in the second zone of next nearest neighbours (NNN) N_2 of 12 atoms, and in subsequent zones with $N_j = 12$ atoms. The NN bond distance (R_1) and coordination numbers N_1, as well as the NNN bond distance (R_2) and coordination numbers N_2 can be determined using EXAFS analysis. However, we have to underline here that for coordination numbers greater, then 6 the error induced by EXAFS can be large and XANES models are more suitable to identify such large coordination numbers.

When the starting two or more binary compounds crystallize in a common B3 or B4 structure, the resulting multinary alloy retains

* Corresponding authors.
E-mail address: andrzej.kisiel@uj.edu.pl (A. Kisiel).

http://dx.doi.org/10.1016/j.opelre.2017.06.012
1896-3757/

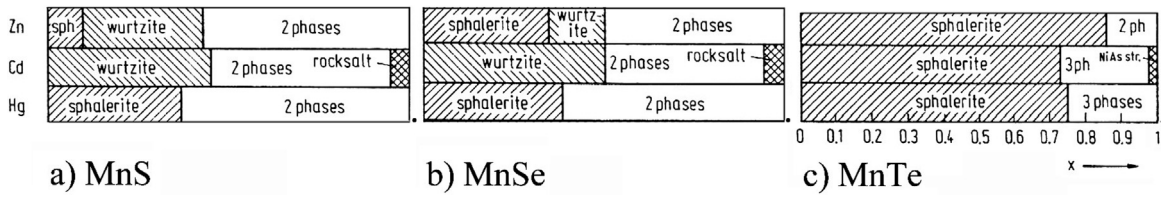

Fig. 1. a) MnS; b) MnSe; c) MnTe solubility of Mn in II–VI for Zn, Cd, and Hg.

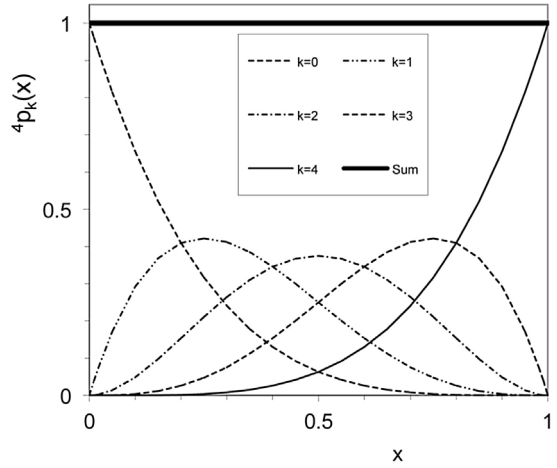

Fig. 2. Bernoulli random distribution $^4p_k(x)$ of elementary configuration tetrahedra in a ternary $A_{1-x}B_xC$ crystal.

the same crystalline structure. If the binary constituents have different crystalline structures, the resulting structure retains the starting structure until a relative content exceeds a value beyond which a structural phase transition occurs, eventually ending with another structure or with a mixture of different structures. This is the typical behaviour of alloys of binary Group II–VI with transition metal (e.g., Mn, Fe, etc.). Transition metal chalcogenides (S, Se, and Te) crystallize in either a six fold coordinated cubic rock salt structure (MnS, MnSe) or in NiAs hexagonal structures (MnTe, FeS, FeSe, and FeTe) (Fig. 1) [1].

For more complex alloys such as quaternary alloys Q_{xy}, we may distinguish two families. The first that we identified as *truly* quaternary with ABCX (Q_{31}) or AXYZ (Q_{13}) formulas consists of fifteen different tetrahedron configurations: 3 binary, 9 ternary, and 3 quaternary while the second described as ABXY(Q_{22}) consists canonically of 4 binary, 12 ternary configurations, and ruling out the presence of antisites has no quaternary. The latter are referred in the next as ***pseudo***-quaternary alloys [2].

2. Analysis of ternary and quaternary semiconductor alloy crystal local structures

Mikkelson and Boyce [3,4] were among the first to investigate semiconductor ternary alloys using EXAFS. They started with the $In_{1-x}Ga_xAs$ ternary zincblende solutions obtained from InAs, successively replacing In by Ga atoms. Using the powder diffraction they observed that the $In_{1-x}Ga_xAs$ lattice constant is linearly dependent on x (Fig. 2a). However, experimental results of EXAFS show that Ga atoms were not substituted at the In atomic positions at the typical distances of the InAs, but were located at distances characteristic of the GaAs binary compound. This surprising behaviour was later explained as the formation of a bi-modal structure in which the different ionic radii of Ga and In cause different R_1's for In-As and Ga-As pairs. In their *Rigid Network Cations* theoretical model Balzarotti et al. [5,6] arbitrarily assumed, the presence in these alloys of a rigid elementary tetrahedron. Cations A and B were rigidly fixed at the corners of the tetrahedron, while the C-anions shifted to a position within the tetrahedron determined by the interactions of AC and BC ions as per the *Force Field Valence* of Keating [7] and Martin [8]. Accordingly, the positions in the elementary tetrahedra named T_0 (4AC), T_1 (3A1BC), T_2 (2A2BC), T_3 (1A3BC) and T_4 (4BC) become a function of the relative content of the alloy (see Fig. 3). Moreover, the model assumes that ions are randomly distributed according to the Bernoulli binomial distribution (Fig. 4) within the five elementary tetrahedra in the crystal. The model was applied to analyze EXAFS data of $In_{1-x}Ga_xAs$ [3,4] $Cd_{1-x}Mn_xTe$ (Fig. 4) [5,6], and $Cd_{1-x}Zn_xTe$ and $HgSe_{1-x}Te_x$ [9]. However, the *Rigid Network Cations* model does not allow a complete description of the EXAFS experimental results of tested ternary alloys. This may be attributed to the fact to the fact that this model disregards obvious deformations of the configuration tetrahedra, due to differences in lattice constants of the two binary components. Part of the shortcomings was removed in the Monte Carlo simulations and in the Modified Quasi Chemical Approximation [10]. Using this model Wiedmann et al. [11] developed the elements of the theory of the *Elastic Stress Relaxation* for ternary alloys $A_{1-x}B_xC$ adding the relaxation of the elemental tetrahedra by the introduction of elementary clusters in the scheme of *Iterative Random Cluster* model.

The statistical *Strained-tetrahedra* model [12,13] is a more precise approach providing an improved description of the structure of ternary and quaternary alloys. The model with its seven axioms covers simultaneously the model of *Rigid Network Cations* and *Cluster* model.

The statistical *Strained-tetrahedron* model was developed to overcome two common assumptions of previous models: 1) rigid undistorted ion sublattice of regular tetrahedra throughout all five configurations and 2) random ion distribution. These simplifying assumptions restrict the range of applicability of the models to a narrow subset of ternary alloys for which the constituent binaries have their lattice constants and standard molar enthalpies of formation ($\Delta_f H_0$) equal or quasi-equal. Beyond these limits predictions of such models become unreliable, in particular, when the ternary exhibits site occupation preferences (SOP).

The seven basic assumptions of the model are:

1) Elemental tetrahedra are free to have different sizes and shapes;
2) All possible (19) elemental inter-ion ternary distances are tetrahedron constrained;
3) Elemental volumes of the two sublattices, for each of the three strictly ternary configurations, pair-by-pair relax to common values, i.e., the three constraints on the distance parameters;
4) Bernoulli binomial polynomials with preference weight coefficients describe configuration populations. ^Np_k (for ternary), $^Np_{kj}$ (for quaternary);
5) All NNN and further fills are determined by NN preferences;
6) Total coordination number is conserved as dilution varies imposing bonds on the coefficient values;
7) The formation of each ternary configuration is carried out until the full consumption of one of the corresponding binary ingredients, or both simultaneously as in the random case, is achieved.

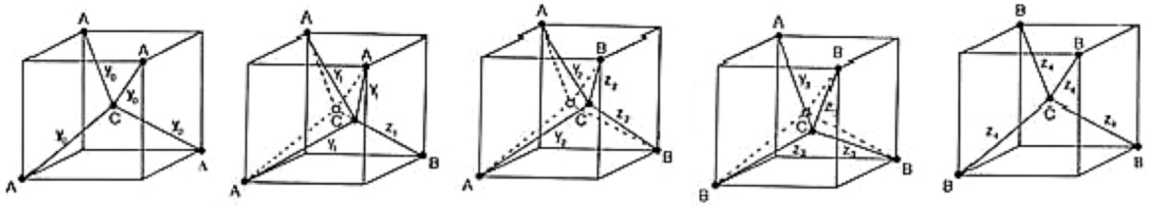

Fig. 3. Rigid Network Cations five elemental tetrahedron configurations $[T_k]_{k=0,4}$ of ABC ternary alloys. Black points and solid lines refer to undistorted tetrahedra; open points and dashed lines show the position of the anion C and bound ions in the distorted case.

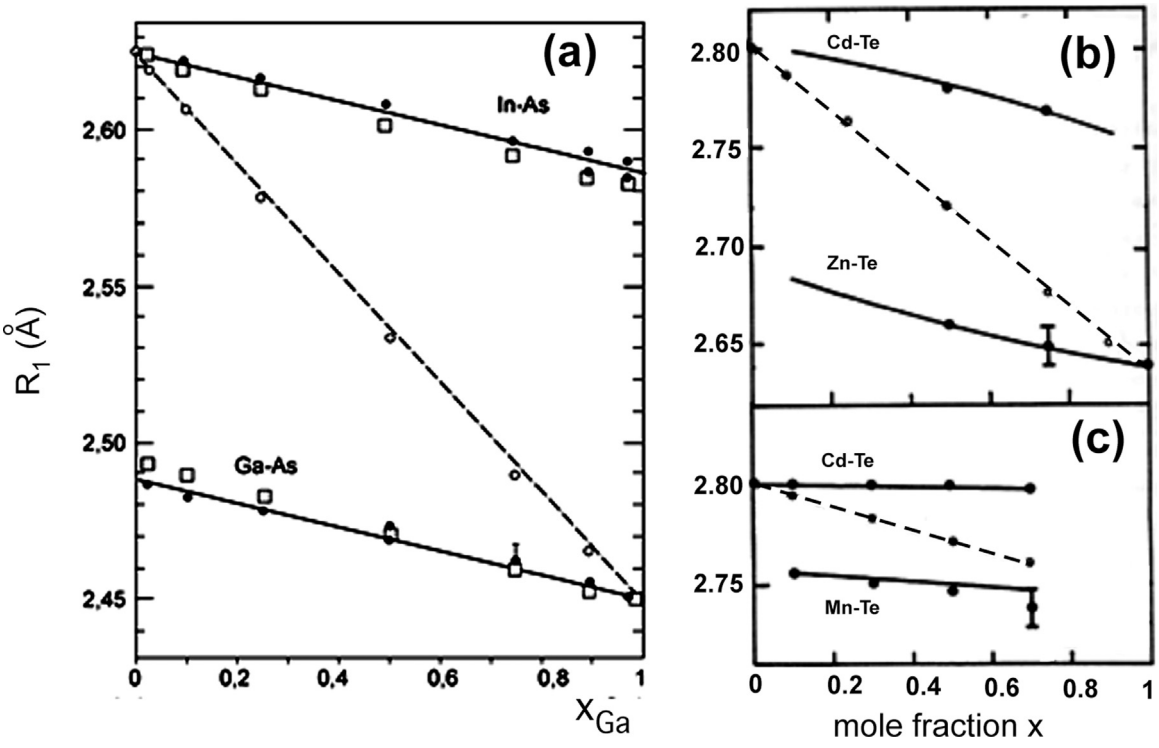

Fig. 4. Analysis of EXAFS structures of: (a) In1-xGaxAs: bond distances R1 In – As and Ga – As as a function of the relative content xGa. Points – experimental results, empty squares – theoretical predictions of the rigid network cation model, dashed line – Vegard line. (b) Cd1-xZnxTe: bond distances R1 of Cd – Te and Zn – Te as a function of the relative content xZn and (c) Cd1-xMnxTe: bond distances R1 Cd -Te and Mn – Te as a function of the relative content xMn, Experimental results – small full circles vs. theoretical predictions – solid lines, Vegard lines – solid straight lines.

These axioms limit the number of free parameters of any tetrahedron ternary to at most ten parameters: three are Site Occupation Preferences (SOPs) and not more then seven distance. A preference parameter equal to either of the two extreme values $W_k \in [0;4/k]$ renders evanescent the relative T_k -configuration population; hence the corresponding distance parameters become dummy. Axioms 2 and 3 were confirmed by the experimental observations. Once the three site occupation preference coefficients and at most seven distance parameters are determined, the SOP coefficients and the sizes and shapes of the elemental tetrahedra are fully known.

The number of strained tetrahedra expected in a multinary alloy is described by the probabilities W_k, while the population of configurations is described by the coefficients C_k. In real multinary alloyed crystals the value $C_k < 1$ leads to a preferential attenuation of the population of distorted tetrahedra T_1, T_2 and T_3. Mass conservation rule imposes that the fraction of distorted tetrahedra T_1, T_2 and T_3 that could not form in the crystal growth process, remain as undistorted tetrahedra T_0 and T_4. Thus, the distribution probabilities P_0 and P_4 of binary tetrahedra T_0 and T_4, besides the respective starting Bernoulli Eigen-functions p_0 and p_4 are enhanced by the part of strained tetrahedra that could not be formed in the real crystal. In all cases atoms\ions distribute themselves among the constituent configurations keeping minimum its internal energy. Distorted tetrahedra have a higher internal energies than the undistorted ones. Thus the formation of undistorted tetrahedral at the expenses of the distorted ones leads to a lower internal energy level of the system. These contributions to the distribution probabilities P_0 and P_4 are discussed Ref. [2] and more recently in Ref. [14] (see Fig. 1).

The *Strained-tetrahedra* model was applied to the EXAFS data of many ternary and quaternary compounds. The results of these studies are summarized in Table 1. Fig. 5 presents the NN and NNN

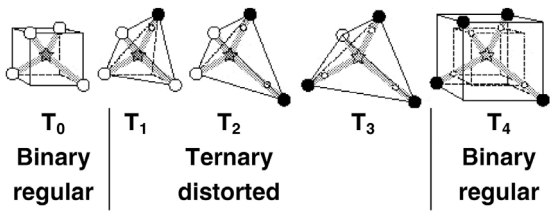

Fig. 5. Strained five elemental tetrahedron configurations $[T_k]_{k=0,4}$ of ABC ternary compounds.

Table 1
Preference parameters of deformed tetrahedra (N = 4) in fcc elementary alloys.

Alloy	Experiment	W_1	W_2	W_3	C_1	C_2	C_3	Sum. C_k	Ref.
ZnCdTe	Exafs [35–37]	1.0	1.0	1.0	1.0	1.0	1.0	3.00	[12]
ZnCdTe	FIR [30,38]	1.66	1	1	0.780	1	1	2.78	[29,38]
CdHgTe	FIR [29,38]	1.01	1.20	1.01	1.0	0.80	1.0	2.80	[29,38]
GaPAs	Exafs [39]	0.93	1.15	1.07	0.930	0.85	0.79	2.57	[12]
ZnCdTe	Exafs [40]	0.93	1.15	1.07	0.930	0.85	0.79	2.57	[12]
ZnCdS	Exafs [41]	0.669	1.044	1.065	0.669	0.956	0.804	2.43	
$AlFeNi_3$	Exafs [32]	1.01	0.86	1.33	0.997	0.86	0.0	1.86	[32]
GaInAs	Exafs [12]	0.58	0.25	1.05	0.58	0.25	0.85	1.68	[12]
CdMnTe	Exafs [5,6]	0.68	1.33	0.003	0.68	0.67	0	1.35	[13]
GaAlN	Exafs [42]	0.03	1.8	1	0.03	0.2	1	1.23	[43]
CdTeSe	Exafs [44]	2.384	0.341	0.262	0.539	0.341	0.262	1.14	
ZnMnSe	Exafs R_1 [31]	0.67	1.67	0.04	0.67	0.33	0.04	1.04	[13]
ZnMnSe	Exafs N_1 [31]	0.62	1.7	0	0.62	0.3	0	0.92	[13]
HgSeTe	Exafs [40]	0.217	1.944	0.517	0.217	0.056	0.517	0.79	
ZnHgTe	FIR [29,38]	0.76	2.0	1.33	0.76	0.0	0.0	0.76	[29,38]
ZnMnS	Exafs [45–47]	1.78	0	0.01	0.74	0	0.01	0.75	[13]
HgMnTe	Exafs [48]	0.33	1.75	0	0.33	0.25	0	0.58	[13]
ZnHgTe	Exafs [49]	0.37	2.0	1.33	0.37	0.0	0.0	0,37	[29,38]
ZnBeSe	Exafs [50]	0	0.255	1.324	0	0.255	0.029	0.28	
ZnMnTe	Exafs [51]	0.37	2.0	0	0.37	0.0	0	0.37	[13]
ZnSeS	Exafs [52]	0.12	0	0.03	0.12	0	0.03	0.15	[52]
ZnSeTe	Exafs [53] & N-Scater [54]	0.037	0	1.299	0.037	0	0.103	0.14	
ZnCdSe	Exafs [55]	4	1.985	0.024	0	0.015	0.024	0.04	

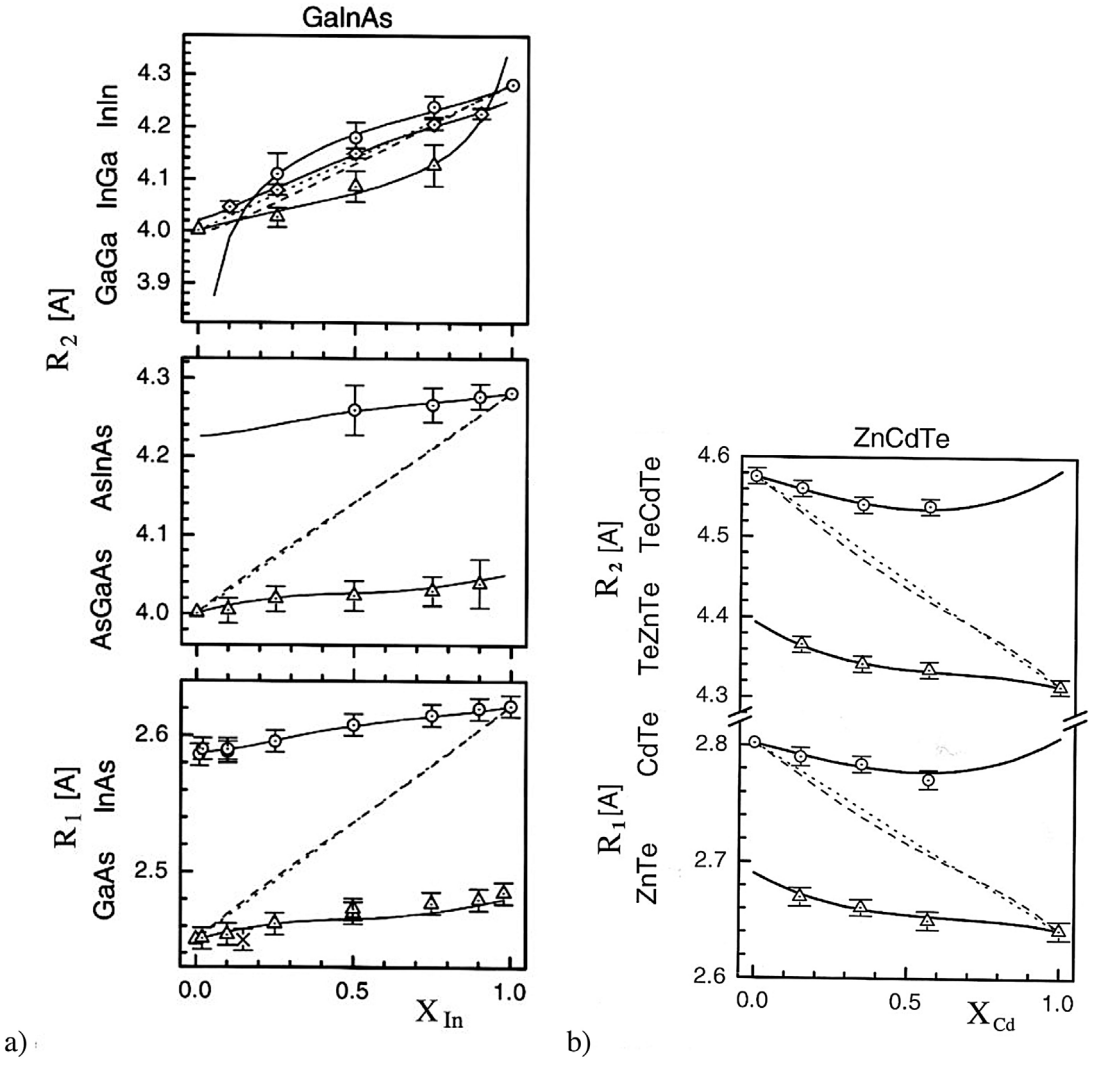

Fig. 6. NN and NNN bond distances R_1 and R_2 of a) $Ga_{1-x}In_xAs$ and b) $Cd_{1-x}Zn_xTe$ as determined using the *Strained-tetrahedron* model.

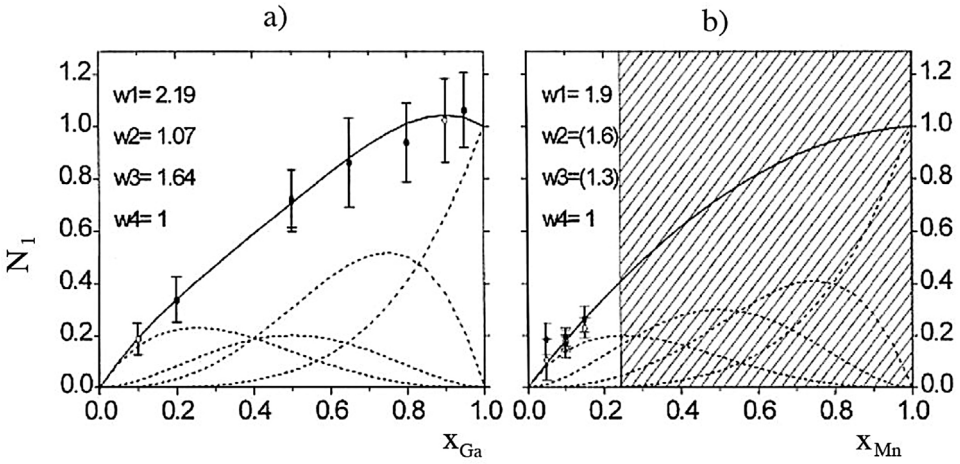

Fig. 7. Fourth-power polynomial best fit of experimental points of a) $Ga_xIn_{1-x}As_{0.05}Sb_{0.95}$ and b) $Cd_xMn_{1-x}Te_{0.1}Se_{0.9}$ with four W_k coefficients.

bond distances R_1 and R_2 of $Ga_{1-x}In_xAs$ and $Cd_{1-x}Zn_xTe$ [12,13]. The model accounts for the deviation from the random distribution in the elementary tetrahedra resulting in a better fit than that obtained by the *Rigid Network Cations* model. This statistical model was developed to overcome two assumptions of the early models: 1) the *rigid undistorted ion sublattice* of regular tetrahedra throughout all five configurations and 2) the random ion distribution. These two simplifying assumptions restrict the range of applicability of the models to a narrow subset of ternary alloys for which the constituent binaries have their lattice constants and standard molar enthalpies of formation (Δ_fH_0) almost equivalent or equal. Outside this condition, predictions are not reliable, in particular, when ternary alloys exhibit site occupation preferences (SOP).

3. Internal preferences in ternary and quaternary compounds

Verleur and Barker [15,16] were first to report on site SOP of atoms in a crystal structure of ternary compounds, using far-infrared (FIR) frequency and intensity of transverse optical (TO) phonons for $GaAs_yP_{1-y}$ and $CdSe_yS_{1-y}$. The theoretical model assumed the clustering parameter β to fit the experimental data taking into account the microscopic scale clustering effect of ion pairs, leading to the distribution of atoms within the crystal. This theoretical approach was applied in several later works concerned with the frequency distribution of vibration and intensity of TO phonons of $Cd_{1-x}Hg_xTe$ [17], $Cd_{1-x}Mn_xTe$ [18], $Cd_{1-x}Zn_xTe$ [19] and $CdSe_xTe_{1-x}$ [20].

EXAFS studies first observed SOPs of atoms in quaternary $Ga_xIn_{1-x}As_ySb_{1-y}$ [21], and preferences for the Ga-As ion pair pairs were reported Fig. 6.

Onabe [22] analyzed the thermodynamic properties of Group III–V quaternary alloys, showed that preferences disrupting the random distribution of pairs of atoms could be attributed to short-range clustering of pairs characterized by a strong bond. Binding pairs can be described by the chemical potential μ. In the case of the $Ga_xIn_{1-x}As_ySb_{1-y}$ we have: $\mu_{GaAs} + \mu_{InSb} > \mu_{InAs} + \mu_{GaSb}$. Preferential site occupations have also been observed with EXAFS at the K-edges of Mn and Se in the $Cd_xMn_{1-x}Te_ySe_{1-y}$ quaternary alloys [23,24]. The study covered the compositions $x < 0.2$ and $y < 0.2$ within which the alloy crystallizes in the zincblende structure, while outside these ranges a multiphase system appear. For these quaternary systems a strong departure from the random distribution of Mn around Se have been observed, which defines the preferences for Mn-Se pairs (Fig. 7). To describe this deviation in both $Ga_xIn_{1-x}As_ySb_{1-y}$ [21] and $Cd_xMn_{1-x}Te_ySe_{1-y}$ [23,24] a probabilistic analysis was used taking into account the best fit of experimental points [38]. In Fig. 7 continuous lines are the best fit of experimental data. The coefficients of the *polynomial* best-fit yields the population probabilities W_k of ion pairs in the tetrahedron configurations T_k [25], with no need of clustering of ion pairs.

The *Strained-tetrahedra* model [12,13] served also to interpret the pseudo quaternary $Ga_xIn_{1-x}As_ySb_{1-y}$ [21] and $Cd_xMn_{1-x}Te_ySe_{1-y}$ [23,24], as well as the truly quaternary $Zn_xCd_yHg_{1-x-y}Te$ [26] and $InAs_xP_ySb_{1-x-y}$ [27]. For the latter, W_k and C_k values are identified by two subsets W_{kj} and C_{kj} [2]. More than a decade ago, the theoretical *Statistical* model started to be developed [28] to interpret also FIR observations of transverse optical (TO) frequencies and intensities or oscillator strengths (OS) [28]. Several ternary alloys (ZnCdTe [2,29], CdHgTe and ZnHgTe [29]) and quaternary alloys [2] ($Cd_xMn_{1-x}Te_ySe_{1-y}$ [25] and $Zn_xCd_yHg_{1-x-y}Te$ [26] were analyzed. The theoretical *Statistical* model successfully compared information derived from the FIR frequency and intensity of phonon vibration spectra to the information obtained by EXAFS. *Strained-tetrahedra* model applied to EXAFS observations and *Statistical* model applied to TO phonon spectra, allow the quantification and the comparison of SOPs of elementary tetrahedron sites in crystals (Table 1). *Strained-tetrahedra* model analysis of EXAFS observations and the *Statistical* model of FIR spectra analysis of TO phonons allow comparing results obtained by these independent methods, are in fair agreement.

Bunker [30] and Pong et al. [31] analyzed distortions in ternary $Zn_{1-x}Mn_xSe$ alloy crystals and carried out a detailed study of NN and NNN neighbours at both room temperature and liquid nitrogen. They determined bond-angles in the deformed elementary tetrahedral and presented a detailed analysis of the numbers of coordination N_j (equation-2.55) at Zn, Mn and Se K-edges. They observed (Fig. 8) that the coordination number of Zn–Zn pairs are slightly lower than that expected for a random distribution (dashed line on Fig. 8) while those for Zn-Mn pairs are slightly higher. They attributed the differences to an incomplete relaxation of stresses in the second coordination zone. Pong et al. [31] data were analyzed using the *Strained-tetrahedra* model [12,13] and pointed out clear internal preferences in $Zn_{1-x}Mn_xSe$ crystals (see Table 1).

In general, depending on how different the original properties of the binary components are site occupation preferences (SOPs) are observed with a distribution of ions\atoms differing from the random Bernoulli values. This is described attributing to each Bernoulli Eigen-function (p_k) a SOP multiplicative factor (C_k) for each tetrahedron configuration (T_k), which describes how the distribution is depressed respect to the expected Bernoulli behavior.

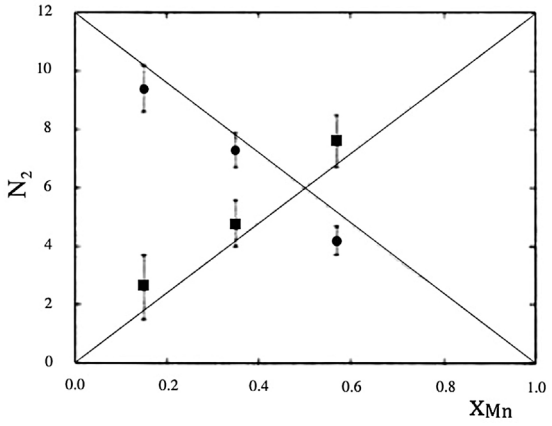

Fig. 8. Coordination numbers N_2 of Zn (solid circles) and of Mn (solid squares) in $Zn_{1-x}Mn_xSe$; (lines) – N_2 for a random distribution of Zn and Mn.

In a configuration with N nearest neighbor (NN) sites to be filled, this probability coefficient W_k ranges:

$$0 \le W_k \le N/K \text{ for } K = 1, 2, \ldots, N-1, \quad (1)$$

for a tetrahedron structured sphalerite or wurtzite, with four NN sites (N = 4)

$$0 \le W_1 \le 4 \quad 0 \le W_2 \le 2 \quad 0 \le W_3 \le 4/3 \quad \text{for } K = 1, 2, 3. \quad (2)$$

$W_k \neq 1$, implies that there are too many preferred ($W_k > 1$) of one type, versus too little ($W_k < 1$) of the other, with the minor population setting a limit to the formation of the multinary, while the excess of preferred contribute to the unused non-distorted binary.

The distribution probability defined by:

$$\{P_k\} = \left\{W_k p k^{/>}\right\} \quad \text{for } k = 1, 2, \ldots, N-1 \quad (3)$$

For the NN population configurations we may write

$$C_k = \min[W_k, 1, (N - kW_k)/N - k] \le 1. \quad (4)$$

Thus, probability distributions of strained tetrahedra T_k in real crystals are attenuated respect to the random Bernoulli distribution p_k. In fact, in the strained tetrahedron model the C_k coefficients representing the attenuation factors of the Bernoulli's Eigen-functions, describe the distributions in the multinary configuration strained tetrahedra, while the W_k's determine the amounts destined to remain as unused binaries.

The ion\atom distributions in multinary fills are depressed respect to the random Bernoulli fill:

$$\{P_k\} = \{p_k\} \quad \text{for } k = 0, 1, \ldots, N \quad (5)$$

splits, in case of preferences into

$$\{P_k\} = \{C_k * p_k\} \quad \text{for } k = 1, \ldots, N-1 \quad \text{while}$$

$$P_0 = po + \Delta po \quad (6)$$

$$P_n = PN + \Delta_{PN}$$

where

$$\Delta p_0 = \Sigma_{k=1,3}[\max(0, 1 - W_k)p_k]$$

$$\Delta p_N = \Sigma_{k=1,3}[\max(0, k(W_k - 1)/(N - k))p_k]$$

To estimate the overall contribution over the full relative content range $x \in [0,1]$ of the IP preferences, we define:

$$^{\Delta N}P_0 = \int \Sigma_{k=1,3}[\max(0, 1 - W_k)^N p_k]dx \text{ and}$$

$$^{\Delta N}P_N = \int \Sigma_{k=1,3}[\max(0, k(W_k - 1)/(N - k))^N p_k]dx.$$

As

$$\int^N p_k dx \equiv 1/(N + 1)$$

we have

$$^{\Delta N}P_0 = \Sigma_{k=1,3}[\max(0, 1 - W_k)]/(N + 1) \text{ and}$$

$$^{\Delta N}P_N = \Sigma_{k=1,3}[\max(0, k(W_k - 1)/(N - k))]/(N + 1). \quad (7)$$

This applies to any crystal structures N = 2 (C15), 4 (B3, B4 $L1_2$), 6 (B2) and 8 (B1).

Equation (4) implies that in case of SOPs, the coefficients C_k are less than unity, i.e., the distributions deviate from the Bernoulli random distribution (Fig. 9). For instance, the SOPs of

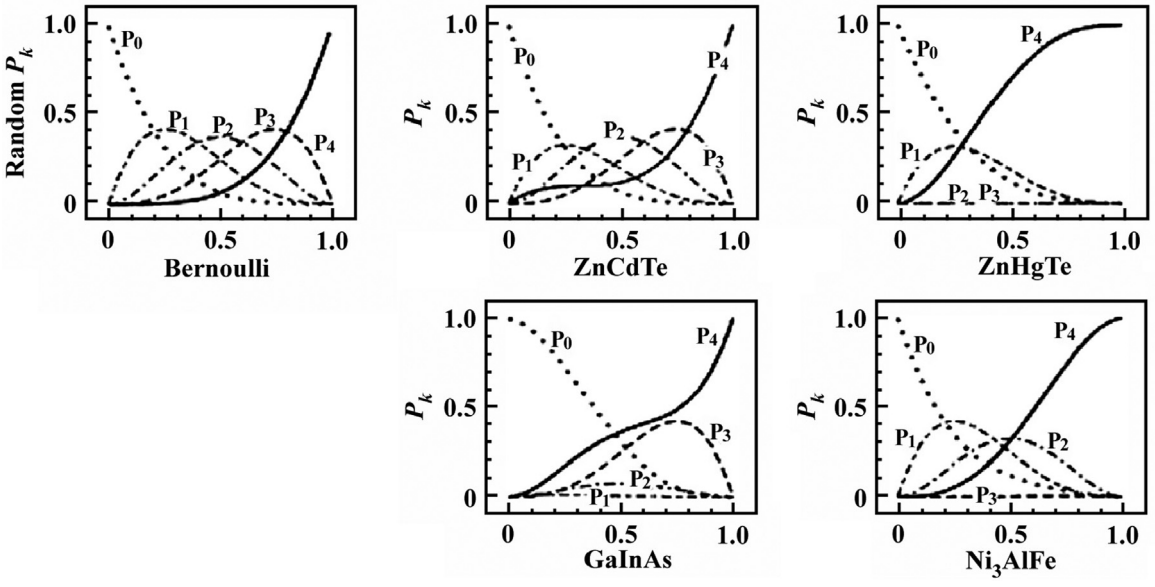

Fig. 9. Population tetrahedron configuration distributions for random Bernoulli p_k, and for P_k associated to ZnCdTe, ZnHgTe, GaInAs and Ni_3AlFe.

Table 2
Preferences in ternary alloys EXAFS\FIR observed.

Group II–VI ternary	Alloy	Method	$^{\Delta N}P_0/(N+1)$	$^{\Delta N}P_N/(N+1)$	Preference
	ZnCdS	EXAFS [41]	0.07	0.05	ZnS > CdS
	ZnBeSe	EXAFS [50]	0.35	0.32	ZnSe > BeSe
	ZnCdSe	EXAFS [55]	0.20	0.66	ZnSe < CdSe
	ZnCdTe	FIR [29]	0.01	0.07	ZnTe < CdTe
	ZnCdTe	EXAFS [12]	0.01	0.12	ZnTe < CdTe
	ZnHgTe	EXAFS [49]	0.13	0.66	ZnTe < HgTe
	ZnHgTe	FIR [29]	0.05	0.67	ZnTe < HgTe
	ZnSeS	EXAFS [52]	0.38	0.32	ZnSe > ZnS
	ZnSeTe	EXAFS [54]	0.35	0.33	ZnSe > ZnTe
	ZnSeTe	EXAFS [54]	0.39	0.30	ZnSe > ZnTe
	CdSeTe	EXAFS [44]	0.19	0.27	CdSe > CdTe
	HgSeTe	EXAFS [40]	0.25	0.31	HgTe < HgSe
Group III–V ternary	GaInAs	EXAFS [12]	0.11	0.10	GaAs > InAs
	GaAlN	EXAFS [42]	0.19	0.27	GaN < AlN
	GaAsP	EXAFS [39]	0.01	0.12	GaAs < GaP
Group II–VI ternary with manganese	ZnMnS	EXAFS [13]	0.40	0.09	ZnS > MnS
	ZnMnSe	EXAFS (N_1) [31]	0.26	0.22	ZnSe > MnSe
	ZnMnSe	EXAFS (R_1) [31]	0.26	0.13	ZnSe > MnSe
	ZnMnTe	EXAFS [51]	0.35	0.33	ZnTe > MnTe
	CdMnTe	EXAFS [5,6]	0.26	0.11	CdTe > MnTe
	HgMnTe	EXAFS [48]	0.33	0.25	HgTe > MnTe
Non B3 B4 alloys	$CeLaRu_2$	EXAFS [33]	0.31	0	$CeRu_2 > LaRu_2$
	$AlFeNi_3$	EXAFS [32]	0.11	0.10	$AlNi_3 > FeNi_3$

the $Zn_{1-x}Mn_xSe$ are $\{W_1, W_2, W_3\} = \{0.67, 1.67, 0\}$ while SOP-coefficients $\{C_{k,k=1,3}\} = \{0.67, 0.33, 0.0\}$, i.e., the T_1 and T_2 tetrahedra are attenuated, while T_3 tetrahedra are not formed. A lack of configuration T_3 has been observed in ternary compounds of Group II–VI containing manganese atoms (Table 1).

The *Strained-tetrahedra* model [12,13] was successfully used to analyze EXAFS data of semiconductor ternary alloys, as well as the cubic (fcc) intermetallic $Ni_3Al_{1-x}Fe_x$ $L1_2$ system [32], and the C15 structured superconductor $Ce_{1-x}La_xRu_2$ [33], illustrating the applicability of the model to structures other than B3 and B4 tetrahedral coordination. In Fig. 9 we compare experimental data of the populations of the ZnCdTe, ZnHgTe, GaInAs and $Ni_3Al_{1-x}Fe_x$ alloys with the random Bernoulli distribution. Table 1 summarizes the values of W_k and C_k as determined from EXAFS and FIR data of sphalerite B3 and wurtzite B4 Group III–V, II–VI alloys with Mn chalcogenides and of the intermetallic $Ni_3Al_{1-x}Fe_x$ with $L1_2$ symmetry.

Initially the distributions were approximated by the Bernoulli Eigen-functions p_k. This turns out to be a good approximation for alloys like ZnTe and CdTe forming the ZnCdTe, while it fails in the extreme case of ZnS and ZnSe forming the ZnSeS. For the latter, site occupation preferences (SOPs) prevent the formation of ternary configurations, leaving an almost bi-binary homogeneous alloy, with but very small contribution of the multinary configurations formed.

Table 1 reports W_k, C_k and ΣC_k values obtained from the strained tetrahedron model analysis of EXAFS, neutron scattering, and FIR data of ternary alloys as available in the literature. The comparison of C_k values in Table 1 indicate which distorted tetrahedra are more or less preferred in the formation of a given ternary alloy. This is the first attempt to determine the Internal Preference (IP) of a real crystal structures. The last column of Table 1 presents the values of $\Sigma C_k \in [0,3]$. A value of 3 corresponds to a random distribution of the strained tetrahedra T_1, T_2 and T_3 well described by the Bernoulli Eigen-functions p_k. This is the case of ZnTe and CdTe forming ZnCdTe with a value $\Sigma C_k \approx 3$. In contrast we have ZnSeS with $\Sigma C_k \approx 0$, an alloy characterized by a very low population of strained tetrahedron configurations with crystals formed mainly with the elemental tetrahedra T_0 and T_4. Most ternary alloys show intermediate values of ΣC_k due to a differentiated attenuation of the distorted tetrahedral contributions.

For sake of simplicity, the population probabilities of elemental tetrahedra T_0 and T_4 (Eq. 6) are $P_0 = p_0 + \Delta p_0$ and $P_N = p_N + \Delta p_{N=4}$, respectively where Δp_0 and $\Delta p_{N=4}$ represent the part of the probability distribution for the undistorted tetrahedra AX and BX of the ternary alloy ABX which, due energy minimization in the growing crystal, could not be created as distorted tetrahedra T_1, T_2 and T_3. The same is true for AX and AY in ternary alloys AXY. The comparison of the complete distribution probabilities P_0 and P_4 returns another IP relation of real crystals.

Fig. 9 shows the population probability distributions for ZnCdTe, ZnHgTe, GaInAs and $Ni_3Al_{1-x}Fe_x$ alloys based on experimental data and compared to the random Bernoulli distribution. Both curves P_0 and P_4 of ternary compounds represent the contribution of the undistorted tetrahedra T_0 and T_4 as the function of composition through the whole ternary compound system. The integrals $^{\Delta N}P_0$ and $^{\Delta N}P_N$ serve to estimate the internal preferences of the non-distorted binary components in the ternary compounds. As shown in Fig. 9 the distribution of P_0 and P_4 function of the relative content of the ternary alloy. The T_0 and T_4 tetrahedron presence in the ternary compound change with content. Thus, the integrated distribution of P_0 and P_4 over the whole composition range indicates the higher or lover participation of binary components in the creation of the ternary compound system. The preferences $\Delta^N P_0$ and $\Delta^N P_N$ are the integrals over the total range of relative content BX in the AX or AX and AY. These internal preferences are given in Table 2.

Table 2 reports normalized $\Delta^N P_0/(N+1)$ and $\Delta^N P_N/(N+1)$ data as calculated on the base of the C_k splitting (Table 1), according to the crystal structures of the binary components of the ternary alloys.

Ternary alloys created from sphalerite or wurtzite binary components undergo no structural phase transition as both binary components AX and BX or AX and AY are alloyed. The analysis of ΣC_k and of probabilities ΔP_0 and $\Delta P_{N=4}$ may give supplementary information. Some ternary alloys exhibit a quasi-random distribution, as ZnCdTe with a slight preference of CdTe over ZnTe as observed from EXAFS and TO phonon analysis. Both GaPAs and CdHgTe exibit too a quasi-random distribution of distorted tetrahedra. On the other hand, both EXAFS and FIR C_k results for ZnCdSe show, an evanescent yet none zero population of distorted tetrahedra. ZnBeSe possesses both T_2 and T_3 distorted tetrahedra with

$C_k \neq 0$, while T_1 tetrahedra are practically absent, with the IP of ZnSe higher than that of BeSe. Generally in II–VI and III–V ternary alloys differences of IP are evident. Some consistent dependence appears in manganese ternary alloys. While binary Group II–VI compounds commonly crystallize as sphalerite or wurtzite tetrahedra binary manganese compounds MnS and MnSe crystallize in octahedral NaCl structures, while MnTe in the hexagonal NiAs structure with non-tetrahedron ordering. Thus as the Mn relative content increases, ternary alloys with manganese start growing as sphalerite until a value beyond which occurs a phase transition to either the structure of the end binary (MnS, MnSe or MnTe) or to some other crystalline multi phase. The phase transition usually occurs at a high Mn content, and the strained-tetrahedron model analysis of the ternary manganese alloys can be correctly applied. EXAFS and FIR observations for ternary alloys with manganese have always been carried out in the homogenous, tetrahedron ordered crystalline region. $Zn_{1-x}Mn_xSe$ [31] has a first phase transition at $x_{Mn} \approx 0.4$ from sphalerite structure to the hexagonal wurtzite structure, both tetrahedron-coordinated. The strained tetrahedral model is applicable in both structure regions. Table 1 shows that for Mn ternary alloys, the C_3 values are either equal to 0 or evanescent. For all reported ternary II–VI with Mn compounds, the II–VI components are preferred in comparison to binaries MnS, MnSe and MnTe. This behaviour is probably directly related to the final phase transition from the tetrahedron-coordinated structure of the ternary alloy to that typical of the manganese chalcogenides.

A similar IP analysis can be applied to quaternary alloys. Truly quaternary alloys, as InAsPSb canonically consist of 3 undistorted binary tetrahedra, 9 ternary distorted tetrahedra and 3 distorted quaternary tetrahedra. A Strained-tetrahedron model analysis of the EXAFS experimental data [34] yields the W_{ij} and C_{ij} values [27], whence the distribution probabilities ΔP_0 and ΔP_N that define the IP of each analyzed material. A complete analysis of the contributions of the ternary and quaternary components of InAsPSb is presently under study [27].

Recently recovered NiAs (B2) structured FeSTe [56] data are being interpreted.

4. Conclusions

The article reviews experimental and theoretical studies for the local crystalline structure of tetrahedron ordered ternary and quaternary semiconductor alloys. Paramount information on the local crystalline structure comes from EXAFS analysis and studies of frequencies and intensities of phonon spectra as well as from neutron scattering analysis. EXAFS experimental data with use of the *Rigid Network Cations* theoretical model and the more elaborate *Strained-tetrahedra* model are analyzed. The analysis, using the *Strained-tetrahedra* model, leads to a deeper understanding of the local crystalline structure; whence the adequacy to use the term of preferences. Also discussed are the phonon spectrum properties, from the time of Verleur and Backer [15,16] first paper, up to the advanced *Statistical* model of Robouch et al. All publications point to the problem of internal preferences, which in the first papers was attributed to ion pairs clustering. The *Strained-tetrahedra* model and *Statistical* model explain internal preferences without the need of ion pair clustering. Both models lead to two kinds of preferences: distribution probability of distorted elemental tetrahedra, and internal preferences between original undistorted elemental binary tetrahedra. Both kinds of internal preferences are quantified by respective coefficients. Actually, while the scenario of quaternary systems is still limited in term of investigated compounds, for ternary alloys departure from the quasi-canonical Bernoulli distributions have been observed in a quite large number of compounds. Indeed, many ternary alloys with B3, B4, $L1_2$ and C15 crystallographic structures are characterized by extreme preferences in which one, several or even all multinary configurations are depressed or lacking indicating a large deviation from the ideal random Bernoulli distribution. The random assumption is not generally fulfilled and has to be checked case by case. However, the still limited dataset does not allow reaching an understanding being impossible to identify a priori an electronic structure leading to extreme preferences. Many questions remain open and deserve further experimental and theoretical investigations in order to clarify the reason why preferences occur in ternary, and more generally in both truly and pseudo multinary alloys.

Peculiar behaviours characterize many of the above technological systems exhibiting a departure from the Bernoulli distribution. As an example, an important singularity in the electron energy spectrum induces a fundamental discontinuity in the phonon frequency temperature dependence of the $Hg_{1-x}Cd_xTe$ alloys [57]. Such singularities could be present in many other compounds where not negligible spin–orbit relativistic contributions may contribute to the chemical bond of these alloys playing a role in the occurrence of extreme pReferences

Acknowledgements

We sincerely acknowledge A. Grilli for his invaluable help in the final setup of the figures of this manuscript.

References

[1] R.R. Galazka, Semimagnetic semiconductors based on HgMnTe and CdMnTe, physics of semiconductors, conf. Ser. 43, in: B.L.H. Wilson (Ed.), Proc. XIV Internat. Conf. Phys. Semiconductors, The Institute of Physics, B., Ed. Edinburgh 1978, 1979, pp. 133–140.
[2] B.V. Robouch, A. Marcelli, M. Cestelli Guidi, A. Kisiel, E. Sheregii, J. Polit, J. Cebulski, M. Piccinini, A. Mycielski, V.I. Ivanov-Omskii, E. Sciesinska, J. Sciesinski, E. Burattini, Statistical model analysis of local structure of quaternary sphalerite crystals, Fiz. Nizk. Temper (ΦHT) 33 (2007) 291–303, Low Temper. Phys., 33 214–225 (2007).
[3] J.C. Mikkelsen, J.B. Boyce, Atomic-Scale structure of random solid solutions: extended X-Ray-Absorption fine-structure study of $Ga_{1-x}In_xAs$, *Phys Rev. Lett.* 49 (1982) 1412–1415.
[4] J.C. Mikkelsen, J.B. Boyce, Extended x-ray-absorption fine-structure study of $Ga_{1-x}In_xAs$ random solid solutions, Phys. Rev. B 28 (1983) 7130–7140.
[5] A. Balzarotti, M. Czyzyk, A. Kisiel, N. Motta, M. Podgorny, M. Zimnal-Starnawska, Local structure of ternary semiconducting random solid solutions: extended x-ray-absorption fine structure of $Cd_{1-x}Mn_xTe$, Phys. Rev. B 30 (1984) 2295–2298.
[6] A. Balzarotti, N. Motta, A. Kisiel, M. Zimnal-Starnawska, M.T. Czyzyk, M. Podgòrny, Model of the local structure of random ternary alloys: experiment versus theory, Phys. Rev. B 31 (1985) 7526–7539.
[7] P.N. Keating, Effect of invariance requirements on the elastic strain energy of crystals with application to the diamond structure, *Phys*, *Rev*. 145 (1966) 637.
[8] R.M. Martin, Elastic properties of ZnS structure semiconductors, Phys. Rev., B 1 (1970) 4005–4011.
[9] A. Balzarotti, M.T. Czyżyk, A. Kisiel, P. Letardi, N. Motta, M. Podgórny, M. Zimnal-Starnawska, EXAFS of $Cd_{1-x}Zn_x$ Te: a test of the random distribution in zincblende ternary alloys, Festkżrperprobleme 25 Adv. Solid State Phys. 25 (1985) 689–6989.
[10] M.T. Czyżyk, M. Podgórny, A. Balzarotti, P. Letardi, N. Motta, A. Kisiel, M. Zimnal-Starnawska, Thermodynamic properties of ternary semiconducting alloys, Zeitschrift Phys B Condensed Matter 62 (1986) 153–161.
[11] M.R. Wiedmann, J.R. Gregg, K.A. Newman, Local structure $Zn_{1-x}Mn_xSe$ alloys, J. Phys. Condens. Matter 4 (1992) 1895.
[12] B.V. Robouch, A. Kisiel, J. Konior, Statistical model for site occupation preferences and shapes of elemental tetrahedra in the zinc-blende type semiconductors GaInAs, GaAsP, ZnCdTe, J. Alloys Compd. 339 (2002) 1–17.
[13] B.V. Robouch, A. Kisiel, J. Konior, Statistical model for atomic distances and site occupation in zinc-blende diluted magnetic semiconductors (DMS's), J Alloys Compd. 340 (2002) 13–26.
[14] B.V. Robouch, C. Marcelli, P. Robouch, A. Kisiel, 'Occupation preference values in doped Cmlm' multinaries from EXAFS and FTIR correlative analysis', Fiz. Nizk. Temper. (ΦHT) (2011) 308–312, Low Temper. Phys., 37, 241–244 (2011).
[15] H.W. Verleur, A.S. Barker, Infrared lattice vibrations in $GaAs_yP_{1-y}$ alloys, Phys. Rev. 149 (1966) 715–729.
[16] H.W. Verleur, A.S. Barker, Optical phonons in mixed crystals of $CdSe_yS_{1-y}$, Phys. Rev. 155 (1967) 750–763.

[17] S.P. Kozyrev, L.K. Vodopyanov, R. Triboulet, Observation of short-order clustering effect in $Hg_{1-x}Cd_xTe$, Solid State Commun. 45 (1983) 383–385.
[18] J.M. Wrobel, B.P. Clayman, P. Becla, R. Sudharsanan, S. Perkowitz, Lattice vibrations of cadmium manganese telluride alloys, J. Appl. Phys. 64 (1988) 310–314.
[19] S. Perkowitz, L.S. Kim, Z.C. Feng, P. Becla, Optical phonons in $Cd_{1-x}Zn_xTe$, Phys. Rev. B 42 (1990) 1455.
[20] S. Perkowitz, L.S. Kim, P. Becla, Infrared analysis of clustering in the II-VI–VI compound $CdSe_xTe_{1-x}$, Phys. Rev. B 43 (1991) 6598.
[21] S.M. Islam, B.A. Bunker, 'Studies of atomic correlations in quaternary semiconductor alloys using the extended X-ray absorption fine structure technique, Phys. Lett. A 156 (1991) 247–252.
[22] K. Onabe, Thermodynamics of type $A_{1-x}B_xC_{1-y}D_y$ III–V quaternary solid solutions, J. Phys. Chem. Solids 43 (1982) 1071–1086.
[23] A. Kisiel, J. Łazewski, M. Zimnal-Starnawska, Manganese distribution in CdMnTeSe crystals. EXAFS data analysis, Acta Phys. Pol. A 90 (1996) 1032–1034.
[24] A. Kisiel, J. Lazewski, M. Zimnal-Stanawska, E. Burattini, A. Myciclski, Site occupation preferences in CdMnTeSe quaternary alloys. EXAFS Data analysis, J. Phys. IV FRANCE C2 (1997) 1997–1998.
[25] B.V. Robouch, A. Kisiel, EXAFS data resolved into individual site occupation preferences in quaternary compounds with tetrahedral coordinated structure, J. Alloys Compd. 286 (1999) 80–88.
[26] E. Sheregii, J. Polit, J. Cebulski, P. Śliż, A. Kisiel, M. Piccinini, A. Marcelli, B.V. Robouch, M. Cestelli Guidi, P. Calvani, V.I. Ivanov-Omskii, First interpretation of phonon spectra of quaternary solid solutions using fine structure far-IR reflectivity by synchrotron radiation, Infrared Phys. Technol. 49 (2006) 13–18.
[27] B.V. Robouch, Hao-Hsiung Lin, R.G. Valeev, J. Omar, P. Robouch, A. Kisiel, A. Marcelli, First Calculation of Site Occupation Preference Coefficients of a Quaternary Alloy: Clear Departure from the Bernoulli Distribution, 2016, in preparation (Private communication).
[28] B.V. Robouch, I.V. Kutcherenko, M. Cestelli Guidi, A. Kisiel, A. Marcelli, P. Robouch, M. Piccinini, A. Nucara, R. Triboulet, E. Burattini, J. Cebulski, E. Sheregii, J. Polit, Ion distribution preferences in ternary crystals $Zn_xCd_{1-x}Te$, $Zn_{1-x}Hg_xTe$ and $Cd_{1-x}Hg_xTe$, Eur. Phys. J. B 84 (2011) 183–195.
[29] B.V. Robouch, I.V. Kutcherenko, M. Cestelli Guidi, A. Kisiel, A. Marcelli, P. Robouch, M. Piccinini, A. Nucara, R. Triboulet, E. Burattini, J. Cebulski, E. Sheregii, J. Polit, Ĭon distribution preferences in ternary crystals ZnxCd1-xTe, Zn1-xHgxTe and Cd1-xHgxTe, Europ. Phys. J. B. 84 (2011) 183–195.
[30] B.A. Bunker, Extended x-ray absorption fine-structure studies of semiconductor structure, J. Vac. Sci. & Technol A: Vacuum, Surfaces, and Films 5 (1987) 3003–3008.
[31] W.F. Pong, R.A. Mayanovic, B.A. Bunker, J.K. Furdyna, U. Debska, Extended x-ray-absorption fine-structure studies of $Zn_{1-x}Mn_xSe$ alloy structure, Phys. Rev. B 41 (1990) 8440–8448.
[32] V.B. Robouch, E. Burattini, A. Kisiel, A.L. Suvorov, A.G. Zaluzhnyi, Strained-tetrahedra statistical model for atomic distances and site occupations in ternary intermetallic M3(X′) structures Ni_3(AlFe) case, J Alloy. Compd. 359 (2003) 73–78.
[33] B.V. Robouch, A. Marcelli, N.L. Saini, A. Kisiel, Statistical model structure of $A_{1-x}Z_xB_2$ Laves phase C15 system-the superconducting alloy $Ce_{1-x}La_xRu_2$, Fiz. Niz. Temper. (ФНТ) 35 (2009) 116–121, Low Temper.Phys., 35, 89–93 (2009).
[34] C.-J. Wu, G. Tsai, Z.-C. Feng, H.-H. Lin, Extended X-ray absorption fine structure of InAsPSb, in: Compound Semiconductor Week (CSW/IPRM), 2011 and 23rd Internat. Conf. on Indium Phosphide and Related Materials, 2011, pp. 1–2.
[35] N. Motta, A. Balzarotti, P. Letardi, A. Kisiel, M.T. Czyzyk, M. Zimnal-Starnawska, M. Podgorny, EXAFS of $Cd_{1-x}Zn_xTe$, a test of the random distribution in zincblende ternary alloys, Solid State Commun. 53 (1985) 509–512.
[36] N. Motta, A. Balzarotti, P. Letardi, A. Kisiel, M.T. Czyzyk, M. Zimnal-Starnawska, M. Podogorny, Random distribution and miscibility of $Cd_{1-x}Zn_xTe$ alloy from exafs, J. Cryst. Growth 72 (1985) 205–209.
[37] M. Podgórny, M.T. Czyzyk, A. Balzarotti, P. Letardi, N. Motta, A. Kisiel, M. Zimnal-Starnawska, Crystallographic structure of ternary semiconducting alloys, Solid State Commun. 55 (1985) 413–417.
[38] B.V. Robouch, A. Marcelli, F. Cordeiro Raposo, P. Robouch, A. Kisiel, L. Di Giambattista, The complex stoichiometry of ternary alloys: what lies beyond the canonical Bernoulli distribution? Solid State Commun. 192 (2014) 75–78.
[39] Z. Wu, K. Lu, Y. Wang, J. Dong, H. Li, C. Li, Z. Fang, 'Extended x-ray-absorption fine-structure study of $GaAs_xP_{1-x}$ semiconducting random solid solutions, Phys.Rev. B 48 (1993) 8694.
[40] P. Letardi, N. Motta, A. Balzarotti, Atomic bonding and thermodynamic properties of pseudo-binary semiconducting alloys, J. Phys. C Solid State Phys. 20 (19) (1987) 2853–2884.
[41] S. Mukherjee A. Nag, P.K. Santra, M. Balasubramanian, S. Chattopadhyay, T. Shibata, F. Schaefers, V. Kocevski, J. Rusz, C. Gerard, O. Eriksson, C.U. Segre, D.D. Sarma, Lattice relaxation in $Zn_{1-x}Cd_xS$ binary alloy: an extended X-ray absorption fine structure (EXAFS) study, Phys Rev. B 89 (2014) (224105-1-11).
[42] K.E. Miyano, J.C. Woicik, L.H. Robins, C.E. Bouldin, D.K. Wickenden, Extended x-ray absorption fine structure study of $Al_xGa_{1-x}N$ films, Appl. Phys. Lett. 70 (1997) 2108–2110.
[43] B.V. Robouch, A. Kisiel, P. Robouch, I. Kutcherenko, L.K. Vodopyanov, L. Ingrosso, A. Marcelli, Local structure analysis of $Ga_{1-x}Al_xN$ epitaxial layer, J. Appl. Phys. 104 (2008), 073508-4 (2008); idem: LNF-04/21 (IR) 15.10.2004 report pp.7.
[44] D.N. Talwar, Z.C. Feng, J.-F. Lee, P. Becla, Structural and dynamical properties of bridgman-grown $CdSe_xTe_{1-x}$ ($0 < x \leq 0.35$) ternary alloys, Phys. Rev. B 87 (2013) (165208-1-12).
[45] M. Zimnal-Starnawska, J. Łażewski, A. Kisiel, F. Boscherini, S. Pascarelli, W. Giriat, EXAFS studies of $Zn_{1-x}Mn_xS$ ternary compounds, Acta Phys. Pol. A 86 (1994) 763–766.
[46] R.J. Iwanowski, K. Lawniczak-Jablonska, I. Winter, J. Hormes, EXAFS studies of local atomic structure in $Zn_{1-x}Mn_xS$, Solid State Commun. 97 (1996) 879–885.
[47] J. Lazewski, M. Zimnal-Starnawska, A. Kisiel, F. Boscherini, S. Pascarelli, W. Giriat, Local structure in $Zn_{1-x}Mn_xS$: EXAFS study, phys. Status Solidi (b) – Basic Res. 197 (1996) 7–12.
[48] R.A. Mayanovic, W.F. Pong, B.A. Bunker, X-ray-absorption fine-structure studies of $Hg_{1-x}Cd_xTe$ and $Hg_{1-x}Mn_xTe$ bond lengths: bond relaxation and structural stability of ternary alloys, Phys. Rev. B 42 (1990) 11174–11182.
[49] A. Marbeuf, D. Ballutaud, R. Triboulet, H. Dexpert, P. Lagarde, Y. Marfaiing, E.X.A.F.S XPS studies of $Hg_{1-x}Zn_xTe$: determination of local atomic structure and valence band maximum, J. Phys. Chem. Solids 50 (1989) 975–979.
[50] T. Ganguli, J. Mazher, A. Polian, S.K. Deb, O. Pages, F. Firszt, An EXAFS study of the structure of the $Zn_{1-x}Be_xSe$ alloy system, J. Phys. 190 (2009), Conference Series (012064-1-012064-4).
[51] N. Happo, H. Sato, T. Mihara, K. Mimura, S. Hosokawa, Y. Ueda, M. Taniguchi, Zn and Te K-edge EXAFS studies of the diluted magnetic semiconductor, J. Phys. Condens. Matter 8 (1996) 4315–4323.
[52] R.G. Valeev, E.A. Romanov, V.I. Vorobiev, V.V. Mukhgalin, V.V. Kriventsov, A.I. Chukavin, B.V. Robouch, Structure and properties of ZnS_xSe_{1-x} thin films deposited by thermal evaporation of ZnS and ZnSe powder mixtures, Mater. Res. Express 2 (2015), 9025006–1-9.
[53] J. Pellicer-Porres, A. Polian, A. Segura, V. Mun˜oz-Sanjoseí, A. Di Cicco, A. Traverse, X-ray-absorption fine-structure study of $ZnSe_xTe_{1-x}$ alloys, J. Appl. Phys. 96 (2004) 1491–1498.
[54] P.F. Peterson, T. Proffen, I.K. Jeong, S.J.L. Billinge, K.S. Choi, M.G. Kanatzidis, P.G. Radaelli, Local atomic strain in $ZnSe_{1-x}Te_x$ from high real-space resolution neutron pair distribution function measurements, Phys. Rev. B 63 (2001) 165211–165217.
[55] F. Loglio, A. Telford, E. Salvietti, M. Innocenti, G. Pezzatini, S. Cammelli, F. D'Acapito, R. Felici, A. Pozzi, M. Foresti, Ternary $Cd_xZn_{1-x}Se$ deposited on Ag (111) by ECALE: electrochemical and EXAFS characterization, Electrochim. Acta 53 (2008) 6978–6987.
[56] N.L. Saini, Nanoscale structure and atomic disorder in the iron-based chalcogenides, Sci. Technol. Adv. Mater. 14 (2013) 12 (014401).
[57] E.M. Sheregii, J. Cebulski, A. Marcelli, M. Piccinini, Temperature dependence discontinuity of the phonon mode frequencies caused by a zero-gap state in HgCdTe alloys, Phys. Rev. Lett. 102 (2009) (045504-1-045504-4).